Available online at www.sciencedirect.com
SCIENCE DIRECT®
Catalysis Today 99 (2005) 329–337
CATALYSIS TODAY
www.elsevier.com/locate/cattod

Desulfurization of digester gas: prediction of activated carbon bed performance at low concentrations of hydrogen sulfide

Andrey Bagreev[a], Sai Katikaneni[b], Sanjay Parab[b], Teresa J. Bandosz[a,*]

[a]*Department of Chemistry, City College of New York, 138th Street and Convent Ave, New York, NY 10031, USA*
[b]*FuelCell Energy, Inc., 3 Great Pasture Road, Danbury, CT 06813-1305, USA*

Available online 15 December 2004

Abstract

Three chemically modified/impregnated activated carbons (supplied by manufactures) were used for adsorption–catalytic removal of hydrogen sulfide from digester gas. The performance of samples was studied in dynamic conditions at 1000, 2000 and 5000 ppm of H_2S in digester gas. The results showed differences in the H_2S removal capacities related to the type of carbon and conditions of the experiment. A decrease in H_2S concentration resulted in an increase in a breakthrough capacity, which is linked to slow kinetics of oxidation process. No significant changes were observed when the oxygen content increased from 1 to 2% and the temperature from 38 to 60 °C. On the surface of carbons studied hydrogen sulfide was oxidized predominantly to sulfur, which was deposited in micropores, either on the walls or at the pore entrances. The capacities at low concentrations, 50 and 100 ppm, of H_2S were determined using an approach based on known theoretical solution of a dynamic model where the parameters of the model were determined from the experimental data at a high concentration of an adsorbate.

Keywords: Activated carbons; Desulfurization; Prediction of capacity; Adsorption/oxidation of hydrogen sulfide

1. Introduction

Nowadays strict environmental regulations are driving force for scientists and engineers to seek efficient and cost effective ways to remove pollutants either from liquid or gaseous phases [1]. Pollutants, besides having detrimental effects on environment and affecting the health of ecosystems, interfere with modern technological processes such as fuel cell operation. In fuel cell, fuel, mainly gaseous, is converted into hydrogen and carbon monooxide on reforming catalysts. Those catalysts very often consist of noble metals on various oxide supports. The presence of even a small quantity of sulfur containing species can 'poison' the catalyst diminishing significantly the efficiency of energy production and feasibility of fuel cell application.

The most common gaseous fuel used in a fuel cell is natural gas. Besides significant amount of methane, it contains sulfur compounds such as hydrogen sulfide and mercaptans on the ppm level. Another inexpensive and environmentally friendly fuel, which can be used as source of hydrogen in the fuel cell, is digester gas. This gas is formed during anaerobic digestion of various organic matters and, as a result of this, it contains 50–5000 ppm of hydrogen sulfide. Other gases present in a digester mixture, which can interfere with a fuel cell operation, are organic halides. All of those compounds should be removed from digester gas before the reforming step takes place.

Leading adsorbents used to remove hydrogen sulfide at ambient conditions are activated carbons [2–28]. To improve their performance, they are generally impregnated with caustic materials such as NaOH or KOH, or otherwise modified [29–35]. The presence of humidity facilitates the surface reaction of H_2S oxidation [20,21,25,26]. The disadvantage of the application of caustic impregnated carbons is their low ignition temperature, which may result in self-ignition of a carbon bed [29]. This caused unmodified activated carbons to become attractive candidates to remove hydrogen sulfide, especially at low concentration in the ppm level. Generally, the process has been studied at two

* Corresponding author. Tel.: +1 212 650 6017; fax: +1 212 650 6107.
E-mail address: tbandosz@ccny.cuny.edu (T.J. Bandosz).

0920-5861/$ – see front matter © 2004 Elsevier B.V. All rights reserved.
doi:10.1016/j.cattod.2004.10.008

Nomenclature

a	adsorption
C	concentration
d	bulk density of adsorbent
k	kinetics coefficient
K_1, K_2	coefficients in Eq. (9)
L	adsorbent bed depth
q	concentration of adsorbate in solid phase
Q	volumetric flow rate
S	cross-sectional area of the empty column
S_{mic}, S_t	specific surface area of micropores and total surface area of adsorbent, respectively
t	time
t_1	dimensionless variable in Eq. (6)
U	velocity of gas in the interstitial spaces
V_{mic}, V_{mes}, V_t	volume of micropores, mesopores and total pore volume, respectively
x	axial coordinate
x_1	dimensionless variable in Eq. (6)
Greek letters	
ε	void fraction in the bed
Subscripts	
b	corresponds to breakthrough conditions
o	inlet of carbon bed
L	outlet of carbon bed
s	saturation conditions

different conditions. One approach uses oxidation of hydrogen sulfide at temperature range from 100 to 250 °C and dry conditions at low oxygen concentration [4–8], whereas another is based on oxidation at a room temperature in the presence of moist air [16–29]. The performance of activated carbons as hydrogen sulfide adsorbents depends on their porosity [19,11–13,25,29] and surface chemistry [25–29]. Pores act as storage space for oxidation products, which are mainly elemental sulfur, sulfur dioxide and/or sulfuric acid. Presence of chemical environment, favorable for dissociation of H_2S enhances adsorption by facilitating its dissociation to HS^- ions, which are further oxidized by active oxygen radicals to polysulfides and sulfur polymers.

So far the commonly used method to study the performance of carbon as hydrogen sulfide adsorbent is ASTM D 6646-01 method [36]. This is an accelerated test in which a carbon bed ($1'' \times 9''$) is exposed to wet air with 10,000 ppm of hydrogen sulfide. The reasons for a high concentration of hydrogen sulfide are very practical. For carbon considered as good, the test time can last from few to tens of hours. Besides the practical point of view and usefulness of the comparison of the results obtained at the same conditions, the accelerated test does not reflect the performance of carbon at a low concentration of hydrogen sulfide. Moreover, the lifetime of the bed can be affected by other species present in the challenge gas, which can be also adsorbed in the carbon pore system. To find the more meaningful capacity value, very often the 'on site' test is needed which is costly and can jeopardize the technological process. The objective of this paper is to present the approach which can be used to predict the capacity of carbon at a low concentration of hydrogen sulfide in the ppm level. To achieve the goal, the detailed studies of activated carbons are performed and the capacities are measured in the accelerated test at various levels of H_2S. That data is used to evaluate the real lifetime of carbons in a desulfurization process, provided that they are going to be exposed to the gas of the same composition.

2. Experimental

2.1. Materials

Three impregnated activated carbons supplied by their manufacturers were used in this study. They are referred to as FCE-2, FCE-4 and FCE-6, and were used as received. After H_2S adsorption an additional letter 'E' is added to the name of the samples.

2.2. Methods

2.2.1. H_2S breakthrough capacity

Moist digester gas (DG: $CH_4 = 60\%$; $CO_2 = 40\%$) (relative humidity: 70% at 38 °C) containing either 5000, 2000 or 1000 ppm of H_2S was passed through the column of adsorbent ($1'' \times 3''$) at 1.65 L/min at atmospheric pressure. The flow rate was controlled using Cole-Parmer flow meters. The residence time of feed gas in the reactor was 0.52 s. The breakthrough of H_2S was monitored using electrochemical sensor. Air was added to keep oxygen inlet concentration in digester gas either 2 or 1 vol.% (small concentrations were chosen arbitrary to have ratio O_2 to H_2S bigger then 2 and they are non-interfering with the fuel cell operation). Gas analyzer downstream of the air–DG mix measured the oxygen concentration, while the RH meter downstream of the bubbler measured the relative humidity. The inlet temperature was maintained either at 38 or 60 °C using an electric heater at the inlet to the reactor bed. A thermocouple downstream of the electric heater measures the temperature and a pressure gage measures the pressure of the DG into the bed. The breakthrough curves were measured at outlet H_2S concentrations of 50, 20 and 10 ppm with inlet concentrations of 5000, 2000 and 1000 ppm, respectively, to keep the constant ratio of the breakthrough concentration to the inlet concentration. The adsorption capacities of each sorbent in terms of milligrams of sulfur containing gases per gram of adsorbent are calculated by integration of the area above the breakthrough curves and from the H_2S concentration in the

inlet gas, flow rate, breakthrough time and mass of adsorbent. Then the breakthrough capacity and life time of adsorbents at challenging gas inlet concentrations 100 and 50 ppm of H_2S were estimated based on mass balance of adsorption–oxidation of H_2S in the dynamic conditions and extrapolation of the data.

2.2.2. pH of carbon surface

The pH of carbon suspension, which provides some information about the average acidity/basicity of adsorbents, was measured in the following way. The sample of 0.4 g of dry carbon powder was added to 20 mL of water and the suspension was stirred overnight to reach equilibrium. Then the pH of suspension was measured.

2.2.3. Thermal analysis

Thermal analysis was carried out using a TA Instruments Thermal Analyzer to determine the products of surface reactions. The instrument settings were: heating rate, 10 °C/min; nitrogen atmosphere with 100 mL/min flow rate.

2.2.4. Sorption of nitrogen

Nitrogen isotherms were measured using an ASAP 2010 (Micromeritics) at −196 °C. Before the experiment, the samples were heated at 120 °C and then outgassed at this temperature under a vacuum of 10^{-5} Torr to constant pressure. The isotherms were used to calculate the specific surface area (S_t), micropores volume (V_{mic}), and total pore volume (V_t). All of the above parameters were calculated using Density Functional Theory (DFT) [37,38].

2.2.5. XRF

X-ray fluorescence analysis was applied to study the sulfur content in carbons. The SPECTRO model 300T Benchtop Analyzer from ASOMA Instruments Inc. was used. The instrument has a titanium target X-ray tube and a high-resolution detector. Company created and calibrated method which allows separation of signals from sulfur and chlorine, was used. The sulfur content was determined using the calibration procedure where mixtures of carbon black with known content of sulfur powder were used as sulfur standards.

3. Results and discussion

The H_2S breakthrough capacity curves carried out on the samples studied at various conditions (different concentration, temperature, and oxygen content) are collected in Fig. 1. From the curves, the breakthrough capacities of adsorbents per mass and unit volume of the carbon bed were calculated. The results are summarized in Tables 1 and 2.

Analysis of the performance of carbons indicates that the capacity of all adsorbents is enhanced when the H_2S concentration decreases. The effect of the temperature does not reveal the common trend due to the various mechanisms

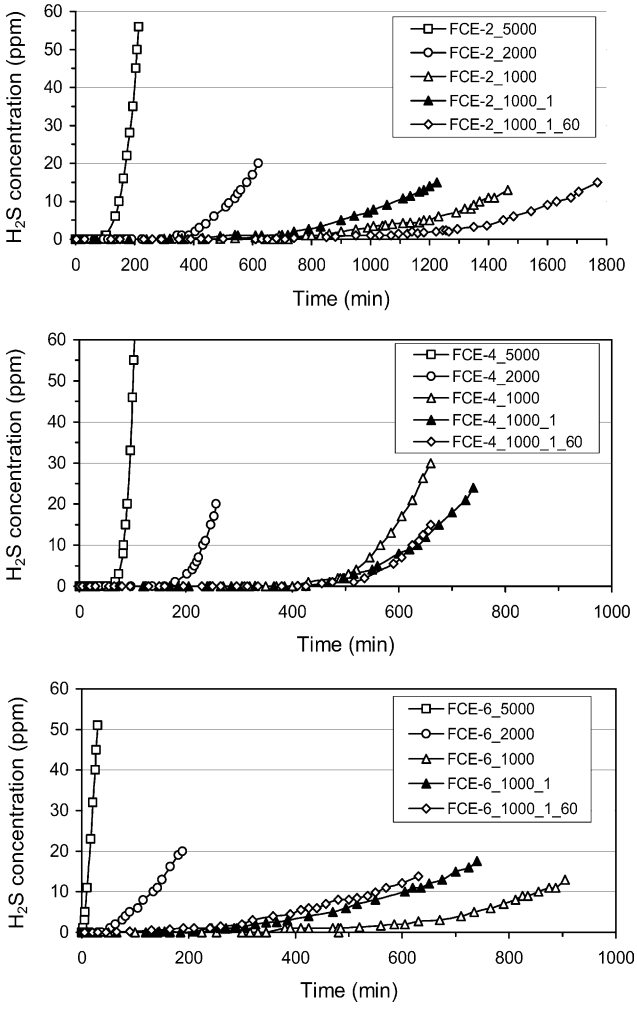

Fig. 1. H_2S breakthrough curves for the carbon samples run at various concentrations. 1 Refers to 1% oxygen content. All samples but that with marked '60', were run at 38 °C.

of oxidation depending on the chemistry of the surfaces [29]. For the best performing sample, FCE-2, an increase in the temperature favors the oxidation process. In the case of the FCE-4 and FCE-6 samples, the effect of temperature is very small. A decrease in the content of oxygen affects the performance of FCF-2 and FCE-6 to the greatest extent (decrease). In the case of FCF-4, 1% oxygen gives slightly better results than 2%. Those changes in the performance are likely governed by the chemistry of the adsorbents' surfaces and the kinetics and dynamics of H_2S adsorption–oxidation from a multicomponent gas mixture. The detailed link between those features is beyond the scope of this paper.

To further check the performance of adsorbents, the emission level of H_2S was measured using a Jerome 631-X Hydrogen Sulfide Analyzer, Arizona Instrument Corporation. After 5 h of the experiments with 1000 ppm of H_2S, 1% O_2 and at 38 °C, the following outlet concentrations of H_2S were detected: 78 ppb for FCE-2, 25 ppb for FCE-4 and 1500 ppb for FCE-6. These results indicate that the highest efficiency of removal exist for FCE-4, the lowest for FCE-6.

Table 1
H_2S breakthrough capacities at various concentrations of H_2S in the challenge gas (2% oxygen, 38 °C)

Sample	5000		2000		1000	
	Breakthrough capacity (mg/g)	Breakthrough capacity (g/cm^3 bed)	Breakthrough capacity (mg/g)	Breakthrough capacity (g/cm^3 bed)	Breakthrough capacity (mg/g)	Breakthrough capacity (g/cm^3 bed)
FCE-2	94	0.054	110	0.064	132	0.076
FCE-4	49	0.027	49	0.027	54	0.029
FCE-6	16	0.009	41	0.019	90	0.044

Table 2
H_2S breakthrough capacities at H_2S concentration in the challenge gas equal to 1000 ppm and 1% oxygen

Sample	1000 ppm	38 °C	1000 ppm	60 °C
	Breakthrough capacity (mg/g)	Breakthrough capacity (g/cm^3 bed)	Breakthrough capacity (mg/g)	Breakthrough capacity (g/cm^3 bed)
FCE-2	100	0.058	158	0.091
FCE-4	63	0.035	62	0.035
FCE-6	65	0.034	64	0.032

Oxidation of H_2S should result in deposition of either sulfur, sulfur dioxide or sulfuric acid on the surface or, if carbon contains impregnants being able to react with H_2S, sulfides or sulfates. The first indication of acid formation is a noticeable decrease in the pH of the carbon surface. The pH values of the samples studied before and after H_2S adsorption with 5000 and 1000 ppm of H_2S in the challenging gas are collected in Table 3. The results show that almost all adsorbents have basic pH, which is favorable for H_2S adsorption. As described elsewhere [25,27,32], the local pH in the pore system greater than pK_{a1} of H_2S enhances hydrogen sulfide dissociation, and thus the oxidation of HS^- ion adsorbed in the film of water. After exhaustion, the pH decreases only slightly suggesting deposition of sulfur as an oxidation product.

One of the methods used here to qualify and quantify the products of surface oxidation is thermal analysis. In this method, it is assumed that the DTG (differential thermal gravimetry) peaks represent desorption of surface reaction products. The amount of those products is linked to the weight loss. As shown previously, sulfuric acid is thermally stable and it desorbs as SO_2 at about 200–300 °C [25–27,40] and at higher temperature polysulfides or elemental sulfur deposited in small pores are removed from the surface. In the case of iron sulfides they are expected to decompose at about 1200 °C [39]. A similar link can be established between the products of methyl mercaptan reaction on carbons (methyl mercaptan, dimethyl disulfide and methanesulfonic acid, etc.). The total amount of adsorbed sulfur can be evaluated based on weight losses in various temperature ranges.

Table 3
Changes in the pH of carbons' surfaces after H_2S adsorption/oxidation

Sample	pH initial	pH E 5000 ppm	pH E 1000 ppm
FCE-2	7.94	7.30	6.35
FCE-4	10.33	9.42	9.01
FCE-6	9.83	9.5	8.40

Fig. 2 shows the comparison of DTG data for the samples studied at various concentrations of H_2S in the challenging gas. For all samples, two peaks are present with maxima between 200 and 300 °C, and 300 and 500 °C. They are related to the removal of the oxidation products. Since the specific information about the speciation of surface oxidation products is beyond the scope of this research, we are not able to assign those peaks to specific compounds (sulfur, sulfuric acid and sulfur containing salts).

It is interesting that while for FCE-4, only slight changes in the thermal desorption are noticed, the changes for FCE-2 and FCE-6 are more complex. For the latter sample, smaller H_2S concentration definitely results in a more intense high temperature peak, which may represent sulfur. For FCE-2, the situation is more complex. The changes in the pH values suggest deposition of some quantity of sulfuric acid, which is likely represented by a sharp peak at 250 °C. This suggests that if elemental sulfur is deposited on the surface of this carbon and it is represented by peaks between 300 and 500 °C [25–27], low concentration of H_2S causes either formation of polysulfides or deposition of elemental sulfur in meso- and macropores, which results in an increase in the intensity of the peak at 300 °C.

Another direct method used to determine the content of sulfur is X-ray fluorescence (XRF). The method is sensitive to the presence of sulfur as element, regardless of its oxidation state. Elemental analysis using XRF involves irradiating a sample with low energy X-ray, causing the elements in the sample to emit their own characteristic X-rays. An X-ray detector then collects the X-rays from the sample so that they can be identified and quantified. The spectra for the samples studied are collected in Fig. 3. The first peak at about 2 keV represents sulfur. For all samples, a significant increase in its intensity is noticed after H_2S

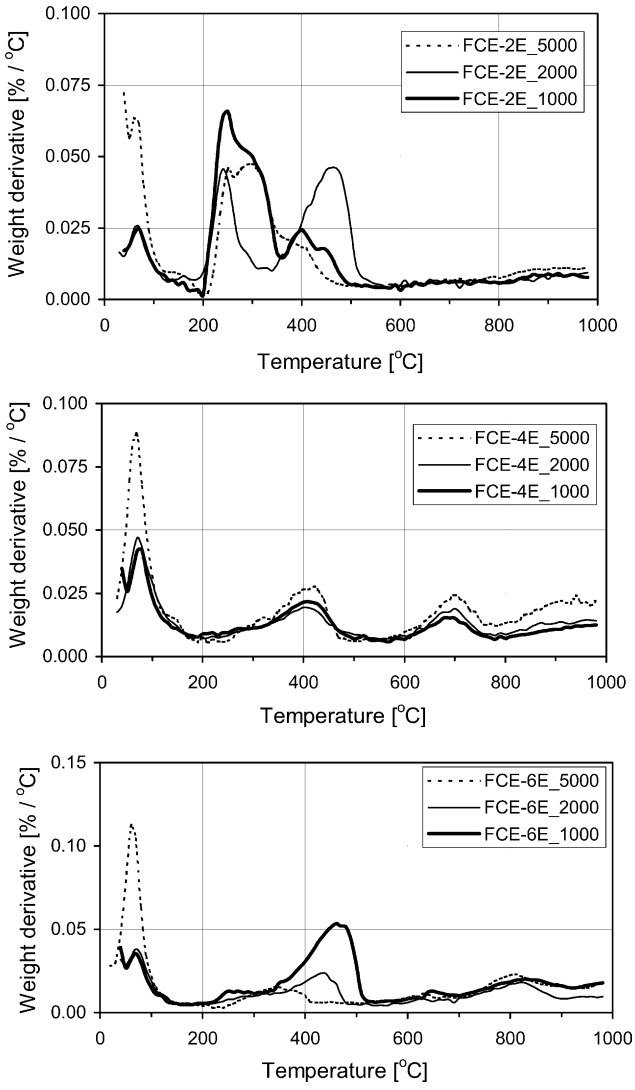

Fig. 2. DTG curves in nitrogen for the samples studied at various concentrations of H_2S in the DG.

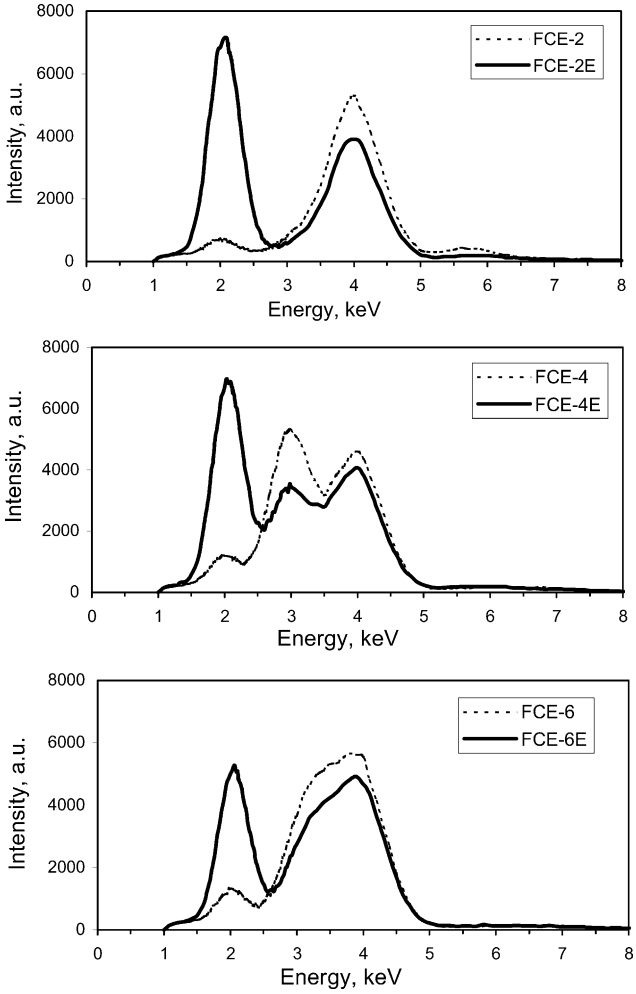

Fig. 3. XRF spectra for initial and exhausted samples.

adsorption. Table 4 presents the comparison of the XRF results and the content of sulfur evaluated from H_2S breakthrough experiments at 5000 ppm of hydrogen sulfide. For all samples, but FCE-6, a relatively good agreement was found.

The oxidation products, if deposited on the surface, should affect the pore structure of the adsorbents. The structural parameters calculated form the nitrogen adsorption isotherms are collected in Table 5. The data obtained after exposure to 1000 ppm of H_2S was chosen to see the most dramatic effect on porosity (the amount adsorbed was the highest at those conditions). Comparison of the initial samples indicates that the most microporous is FCE-2 (the highest degree of microporosity calculated as the ratio of the V_{mic}/V_t) and the degree of microporosity decreases following the order observed in the H_2S breakthrough capacity measurement. The FCE-2 sample has the smallest surface area, which do not have any negative effect on the performance of adsorbent in the process of hydrogen sulfide removal. As expected, after H_2S adsorption, a significant decrease in the structural parameters is noticed, especially for FCE-6, where 56% pore volume becomes inaccessible for the nitrogen molecule compared to about 30% for the other two samples. This is an interesting finding since the performance of this sample as H_2S adsorbent was the worse. The only plausible explanation on this stage of our study is a different mechanism of adsorption/oxidation than that on FCE-6 than on FCE-2 and FCE-4. Apparently sulfur, which is likely the product of H_2S oxidation based on the result described above, deposits at the pore entrances and makes the space inside unavailable for the adsorption process. This mechanism was observed previously on unmodified activated carbons [25,26]. On the other two carbons, especially on FCE-2 where a significant amount of sulfur containing species is deposited on the surface, the catalytic action of the impregnants may be more pronounced resulting in a gradual filling of the pore space combined with deposition at the pore entrances.

Information about the location of surface oxidation products can be obtained analyzing the pore size distributions presented in Fig. 4. Indeed, the differences exist

Table 4
Results of sulfur determination by XRF method in initial and exhausted samples (at 5000 ppm of H_2S in DG)

Sample name	Sulfur content XRF (%)	Sulfur adsorbed H_2S, breakthrough (%)
FCE-2	0.16	–
FCE-2E	7.66	9.06
FCE-4	0.4	–
FCE-4E	7.22	5.04
FCE-6	0.4	–
FCE-6E	4	1.6

between FCE-6 and the other two samples in the pattern how the PSDs are affected after H_2S adsorption–oxidation. It is interesting that for the FCE-6 sample, the volume of all pores decreased, but the changes are the most pronounced for pores smaller than 20 Å, which can be easily blocked by the sulfur deposit. On the other hand, for FCE-2 and FCE-4, the distributions in the range of very small pores become narrower, which suggests deposition of sulfur on the micropore walls. Also the volume of pores between 10 and 20 Å is significantly altered which may be linked to the partial blocking of the pore entrances as in the case of FCE-6.

The data described above is crucial for estimation of H_2S breakthrough time and capacity at 100 and 50 ppm H_2S in the digester gas. The prediction of the breakthrough time and capacities of adsorbents at a very low concentration of H_2S may be done using different approaches [41–43]. The first involves choosing an appropriate theoretical model and calculating the breakthrough curve and capacity from such a model [42,43]. This requires knowing 'a priori' mass transfer coefficients, diffusivity, and the parameters of adsorption isotherm. The second type of approach is completely empirical and based on performing the experiments in appropriate conditions (low concentration, the same hydrodynamic conditions and geometry of the adsorbent bed) and determining the breakthrough time and capacity directly from the experimental data [41].

In our evaluation, we use a combined approach based on known theoretical solution of the adsorption model, where the parameters of model are determined from the experimental data at a high concentration of an adsorbate. Then the breakthrough time for the required conditions is calculated from the extrapolation of the experimental data fitted by the theoretical equation followed from the model.

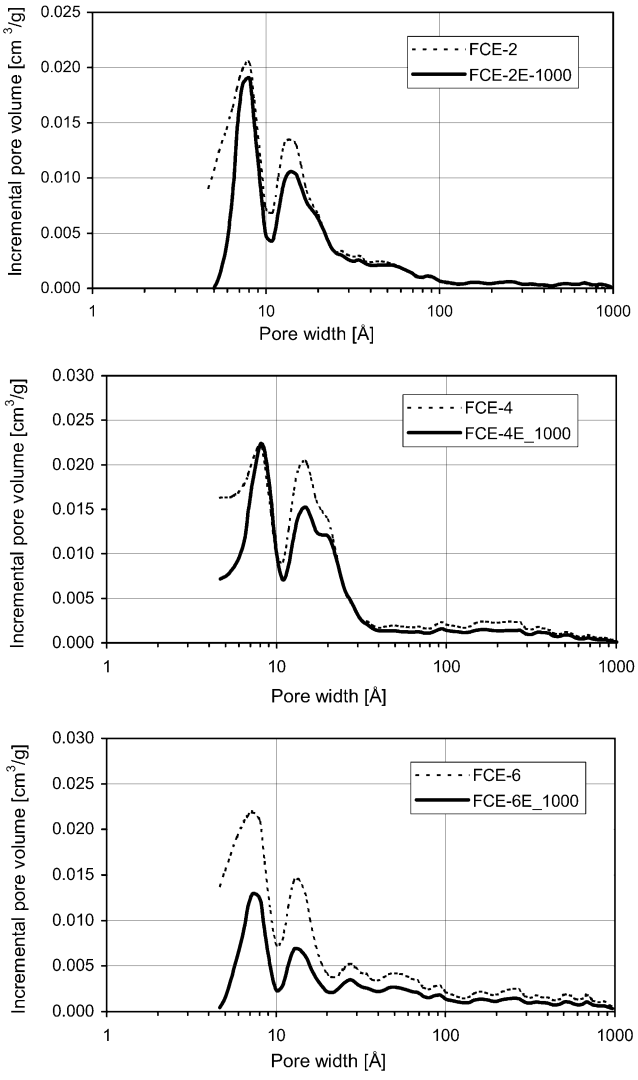

Fig. 4. Pore size distributions for initial and exhausted samples.

The mechanism of removal of H_2S from DG in the presence of oxygen, probably has an adsorption–catalytic nature. It means that reagents, hydrogen sulfide and oxygen, adsorb on the active sites of the solid surface and then catalytically react with formation of elemental sulfur and water, which are then adsorbed in micropores. The process is completely irreversible at temperatures lower then melting point of sulfur. If we assume the isothermal conditions of process, which is correct at a low concentration of H_2S and plug flow of reaction gases in a fixed bed reactor, the

Table 5
Structural parameters for initial and exhausted adsorbents (carbons are exhausted after exposure to 1000 ppm of H_2S in the challenge DG gas)

Sample	S_{BET} (m^2/g)	V_{mic} (cm^3/g)	V_{mes} (cm^3/g)	V_t (cm^3/g)	S_{mic} (m^2/g)	S_t (m^2/g)
FCE-2	692	0.248	0.058	0.321	592	631
FCE-2E	489	0.166	0.055	0.224	345	378
FCE-4	965	0.331	0.104	0.473	766	821
FCE-4E	729	0.255	0.081	0.353	557	603
FCE-6	814	0.273	0.116	0.423	692	756
FCE-6E	346	0.115	0.073	0.194	263	303

following mathematical model may be used to describe the dynamics of adsorption [41–43].

Mass balance (continuity) equation for a fixed bed adsorber:

$$\frac{\partial C}{\partial t}+U\frac{\partial C}{\partial x}+\frac{(1-\varepsilon)}{\varepsilon}\frac{\partial q}{\partial t}=0 \quad (1)$$

Kinetics of adsorption:

$$\frac{\partial q}{\partial t}=kC(q_s-q) \quad (2)$$

Initial and boundary conditions:

$$t=0,\quad C(x)=0;\quad q(x)=0 \quad (3)$$

$$x=0,\quad C(t,x)=C_o \quad (4)$$

Isotherm of adsorption:

$$q=\begin{cases}0, & \text{if } C=0\\ q_s, & \text{if } C>0\end{cases} \quad (5)$$

This model first proposed by Bohart and Adams [44] and widely used to describe the dynamics of adsorption when chemical reaction takes place. Eq. (1) represents the differential mass balance in a fixed bed adsorber with corresponding initial and boundary conditions (3,4). At initial moment of time, $t=0$, the bed is free from adsorbate and reaction products. The concentration of adsorbate in gas phase (C) (in our case H_2S) and adsorbed phase (q) is equal to zero at any point of bed. The inlet concentration of H_2S is constant and equal to C_o, at any moment of time.

The 'quasichemical' rate law (2) is used to describe kinetics of process. Rate of adsorption, $\partial q/\partial t$, is proportional to the concentration of H_2S and to the fraction of adsorbent capacity '(q_s-q)', which still remains at the present moment of time, where q_s is the constant value of q corresponding to the saturation (equilibrium) condition and k is the kinetics coefficient. In this type of a model the rectangular isotherm (5) is widely applied do describe the equilibrium in a system under reaction [43]. It is important to note that 'q' is the average concentration of adsorbate in the solid phase, expressed in the units of mass of adsorbate per unit volume of a solid phase. It is linked to the value of adsorption 'a', which has a dimension of 'gram of adsorbate per gram of adsorbent' in the following expression: $a=q(1-\varepsilon)/d$, where ε is the porosity of the carbon bed and d is the adsorbent bulk density.

For zero axial dispersion, the differential mass balance equation was solved along with the rate expression and rectangular isotherm, and solution can be expressed as [41,42]:

$$\frac{C}{C_o}=\frac{\exp(t_1)}{\exp(t_1)+\exp(x_1)+1} \quad (6)$$

where $x_1=kq_sx\varepsilon/U(1-\varepsilon)$ and $t_1=kC_o(t-(x/U))$ are the dimensionless variables, U is the average axial velocity of the flowing gas mixture in the interstitial spaces, and ε is the void fraction in the bed. If Q is the volumetric flow rate of the gas phase (cm^3/min) and S is the cross-sectional area of the empty column (cm^2), then U (cm/min) is equal to $Q/S\varepsilon$.

Expression (6) allows calculation of the distribution of H_2S through the bed at any moment of time if all parameters of the model are known. To calculate the breakthrough curves one needs to be interested only in the variation of concentration at the end of the bed, namely at $x=L$. For this case a very simple equation is derived for breakthrough time, t_b, of the adsorbent bed with a bed depth is equal to L:

$$t_b=\frac{L}{U}+\frac{(x_L-\ln(C_o/C_b-1))}{kC_o}, \quad (7)$$

where $x_L=kq_sL\varepsilon/U(1-\varepsilon)$ and C_b is the breakthrough concentration.

Applicability of the described model and solution (6) is demonstrated in Fig. 5, where, as an example, the calculated total breakthrough curves are plotted in comparison with the experimental data (points). Calculation was done for the sample FCE-4 and three initial concentrations of H_2S: $C_o=4555$, 1830 and 910 ppm (5000, 2000 and 1000 ppm corrected for the content of oxygen).

The parameters of the model, i.e. a kinetics coefficient (k), and the capacity of an adsorbent (q_s) were found by fitting the theoretical and experimental breakthrough curves for $C_o=910$ ppm and then other two curves were calculated using these parameters without an additional fitting of the data.

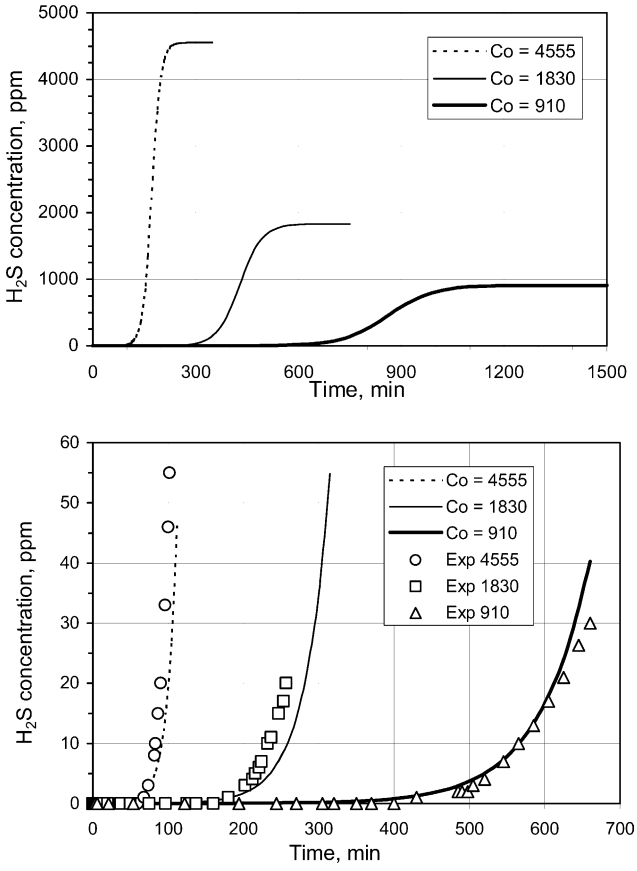

Fig. 5. Predicted (lines) and experimental (points) breakthrough curves for sample FCE-4. Upper plot corresponds to total breakthrough curves and lower to initial part of these curves.

Table 6
Predicted H_2S breakthrough time and capacities of materials studied at 50 and 100 ppm of H_2S in DG

Sample	$K1$	$K2$	Breakthrough time at 100 ppm (h)	Breakthrough time at 50 ppm (h)	Breakthrough capacity at 100 ppm (mg/g)	Breakthrough capacity at 50 ppm (mg/g)
FCE-2	67248	1.17	306	659	206	232
FCE-4	12733	1.06	96	201	68	71
FCE-6	19500000	2.08	1349	5704	1076	2275
FCE-6[a]			691	1382	551	551

K_1 and K_2 are coefficients obtained for fitting the data to Eq. (9).
[a] The prediction done based on the volume of micropores (V_{mic} (DFT)) of adsorbent.

In general, expression (7) may be used to predict the breakthrough time for any inlet concentration if the kinetics coefficient and capacity of adsorbent are known. When these parameters are not known, the next procedure may be applied to predict the breakthrough time at a very low H_2S concentration. We can neglect the first term in Eq. (7) due to its small value in comparison with the second one, and after taking logarithm of both side of Eq. (7) we have:

$$\log(t_b) = \log\left(\frac{x_L - \ln(C_o/C_b - 1)}{k}\right) - \log(C_o) \quad (8)$$

If we 'stabilize' value C_o/C_b at some certain level, for example $C_o/C_b = 100$, and take into account that x_L does not depend on C_o, a linear equation can be obtained:

$$\log(t_b) = K_1 - K_2\log(C_o), \quad (9)$$

where $K_1 = \log((x_L - \ln(C_o/C_b - 1))/k)$ and $K_2 = 1$.

Plotting the experimental data for the breakthrough time versus the initial concentration (Fig. 6) and fitting these data using Eq. (9), one can found coefficients K_1 and K_2 (Table 6). Then the breakthrough time for the low concentration can be easily predicted by extrapolation of the experimental data to 100 and 50 ppm (Fig. 6) or from a direct calculation t_b using Eq. (9) for the concentration of interest. The results of these calculations are collected in Table 6.

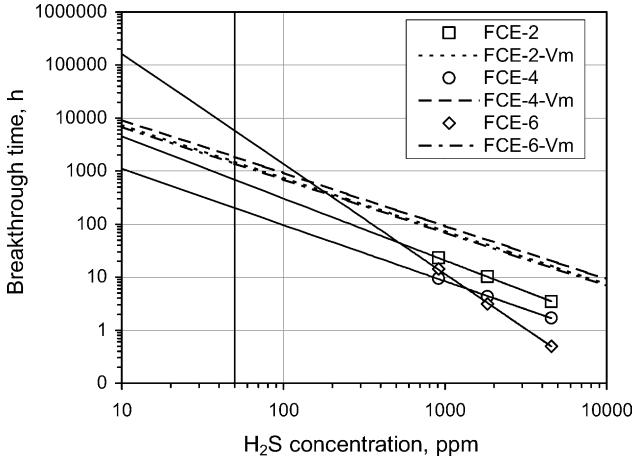

Fig. 6. Dependences of breakthrough time versus inlet concentration of H_2S. Solid lines correspond to fitting of the experimental data to Eq. (9). Dashed lines correspond to limiting breakthrough time calculated from the volume of micropores V_{mic} (DFT).

For all samples except FCE-6 the coefficient K_2 is close to the predicted value, which is 1. In the case of FCE-6 the predicted breakthrough time is unusually big, due to high values of K_1 and K_2. Because of these, a limitation in the amount adsorbed has to be used. It is generally true that the volume of the adsorbed product cannot be greater than the micropore volume, where the adsorption takes place. It follows that in such a case the micropore volume governs the performance of the materials.

4. Conclusions

The results presented in this paper show that the measured capacity of carbon for H_2S removal from digester gas depends on the concentration of hydrogen sulfide. Lower is the concentration, higher is the capacity of adsorbent. Various contents of oxygen (1 or 2%) and an increase in the temperature of the reactor (from 38 or 60 °C) have no significant effect on the performance of the materials. However, the results of the accelerated test (at a high concentration) do not reflect the ultimate capacity of the materials, they can be used to predict the capacity and breakthrough time at very low, ppm levels of H_2S in digester gas. For this evaluation, to make the important assumptions about the nature of the process, the detailed characterization of adsorbents surfaces is needed.

References

[1] S.E. Manahan, Environmental Chemistry, seventh ed. CRC Press, Boca Raton, FL, 1997.
[2] I. Coskun, E.L. Tollefson, Can. J. Chem. Eng. 58 (1986) 72.
[3] M. Steijns, P. Mars, Ind. Eng. Chem., Prod. Res. Dev. 16 (1977) 35.
[4] T.K. Ghosh, E.L. Tollefson, Can. J. Chem. Eng. 64 (1986) 960.
[5] T.K. Ghosh, E.L. Tollefson, Can. J. Chem. Eng. 64 (1986) 969.
[6] A.K. Dalai, M. Majumadar, A. Chowdhury, E.L. Tollefson, Can. J. Chem. Eng. 71 (1993) 75.
[7] A. Yang, E.L. Tollefson, A.K. Dalai, Can. J. Chem. Eng. 66 (1998) 76.
[8] A.K. Dalai, E.L. Tollefson, Can. J. Chem. Eng. 76 (1986) 902.
[9] A.K. Dalai, A. Majumdar, E.L. Tollefson, Environ. Sci. Technol. 33 (1999) 2241.
[10] V. Meeyoo, D.L. Trimm, N.W. Cant, J. Chem. Technol. Biotechnol. 68 (1997) 411.
[11] M. Steijns, F. Derks, A. Verloop, P. Mars, J. Catal. 42 (1976) 87.
[12] M. Steijns, P. Koopman, B. Nieuwenhuijse, P. Mars, J. Catal. 42 (1976) 96.

[13] M. Steijns, P. Mars, J. Catal. 35 (1974) 11.
[14] J. Klein, K.-D. Henning, Fuel 63 (1984) 1064.
[15] K. Hedden, L. Humber, B.R. Rao., VDI-Bericht 253 (1976) 37.
[16] H. Katoh, I. Kuniyoshi, M. Hirai, M. Shoda, Appl. Catal. B 6 (1995) 255.
[17] S. Tanada, T. Kita, K. Boki, Y. Kozaki, J. Environ. Sci. Health A20 (1985) 87.
[18] J.J. Choi, M. Hirai, M. Shoda, Appl. Catal. A 79 (1991) 241.
[19] R. Sreeramamurthy, P.G. Menon, J. Catal. 37 (1975) 287.
[20] A. Primavera, A. Trovarelli, P. Andreussi, G. Dolcetti, Appl. Catal. A: Gen. 173 (1998) 85.
[21] A.N. Kaliva, J.W. Smith, Can. J. Chem. Eng. 61 (1983) 208.
[22] L.M. Le Lauch, A. Subrenat, P. Le Cloirec, Langmuir 19 (2003) 10869.
[23] S.V. Mikhalovsky, Yu.P. Zaitsev, Carbon 35 (1997) 1367.
[24] T.J. Bandosz, Carbon 37 (1999) 483.
[25] F. Adib, A. Bagreev, T.J. Bandosz, Environ. Sci. Technol. 34 (2000) 686.
[26] F. Adib, A. Bagreev, T.J. Bandosz, J. Colloid Interface Sci. 214 (1999) 407.
[27] F. Adib, A. Bagreev, T.J. Bandosz, J. Colloid Interface Sci. 216 (1999) 360.
[28] F. Adib, A. Bagreev, T.J. Bandosz, Ind. Eng. Chem. Res. 39 (2000) 2439.
[29] T.J. Bandosz, A. Bagreev, F. Adib, A. Turk, Environ. Sci. Technol. 34 (2000) 1069.
[30] R. Yan, D.T. Liang, L. Tsen, J.H. Tay, Environ. Sci. Technol 36 (2002) 4460.
[31] H.-L. Chiang, J.-H. Tsai, C.-L. Tsai, Y.-C. Hsu Sep, Sci. Technol. 35 (2000) 903.
[32] A. Bagreev, T.J. Bandosz, Ind. Eng. Chem. Res. 41 (2002) 672.
[33] J. Przepiorski, A. Oya, J. Mater. Sci. Lett. 17 (1998) 679.
[34] J. Przepiorski, S. Yoshida, A. Oya, Carbon 37 (1999) 1881.
[35] J. Przepiorski, Y. Abe, S. Yoshida, A. Oya, J. Mater. Sci. Lett. 16 (1997) 1312.
[36] ASTM Standards, Refractories; carbon and graphite products; activated carbon, Adv. Ceram. 15.01 (1998), ASTM D6646-01.
[37] C.M. Lastoskie, K.E. Gubbins, N.J. Quirke, J. Phys. Chem. 97 (1993) 4786.
[38] J.P. Olivier, J. Porous Mater. 2 (1995) 9.
[39] R.C. Weast (Ed.), Handbook of Chemistry and Physics, seventh ed. CRC Press, Boca Raton, FL, 1986.
[40] J. Rodriguez-Mirasol, T. Cordero, J.J. Rodriguez, Abstract of 23rd Biennial Conference on Carbon, College Park, PA, 1997, p. 376.
[41] D.O. Cooney, Adsorption Design for Wastewater Treatment, Lewis Publishers, Boca Raton, FL, 1999.
[42] M.D. Ruthven, Principles of Adsorption and Adsorption Processes, Wiley, New York, 1984, 430.
[43] R.T. Yang, Gas Separation by Adsorption Processes (Series on Chemical Engineering: vol. 1), Imperial College Press, London, 1987, p. 350.
[44] G.S. Bohart, E.Q. Adams, J. Am. Chem. Soc. 42 (1920) 523.